

# Hydrocarbon analogues of boron clusters — planarity, aromaticity and antiaromaticity

HUA-JIN ZHAI<sup>1,2</sup>, BOGGAVARAPU KIRAN<sup>1,2</sup>, JUN LI<sup>2</sup> AND LAI-SHENG WANG<sup>\*1,2</sup>

<sup>1</sup>Department of Physics, Washington State University, 2710 University Drive, Richland, Washington 99352, USA

<sup>2</sup>W. R. Wiley Environmental Molecular Sciences Laboratory, Pacific Northwest National Laboratory, P.O. Box 999, Richland, Washington 99352, USA

\*e-mail: ls.wang@pnl.gov

Published online: 9 November 2003; doi:10.1038/nmat1012

An interesting feature of elemental boron and boron compounds is the occurrence of highly symmetric icosahedral clusters. The rich chemistry of boron is also dominated by three-dimensional cage structures. Despite its proximity to carbon in the periodic table, elemental boron clusters have been scarcely studied experimentally and their structures and chemical bonding have not been fully elucidated. Here we report experimental and theoretical evidence that small boron clusters prefer planar structures and exhibit aromaticity and antiaromaticity according to the Hückel rules, akin to planar hydrocarbons. Aromatic boron clusters possess more circular shapes whereas antiaromatic boron clusters are elongated, analogous to structural distortions of antiaromatic hydrocarbons. The planar boron clusters are thus the only series of molecules other than the hydrocarbons to exhibit size-dependent aromatic and antiaromatic behaviour and represent a new dimension of boron chemistry. The stable aromatic boron clusters may exhibit similar chemistries to that of benzene, such as forming sandwich-type metal compounds.

**B**oron is only the fifth element in the periodic table and possesses a richness of chemistry second only to carbon<sup>1–6</sup>. However, elemental boron has a huge variety of crystal structures<sup>5,6</sup> compared with the two known to carbon (graphite and diamond). One of the most striking features of elemental boron and many bimetallic solid boron compounds is the occurrence of the B<sub>12</sub> icosahedral clusters<sup>6–8</sup>. The chemistry of boron is also dominated by three-dimensional (3D) cage molecules, such as the well-known B<sub>12</sub>H<sub>12</sub><sup>2–</sup> icosahedron. This is in contrast to the 2D structure exhibited by carbon in graphite, although the fullerenes do possess cage structures. Compared with clusters of carbon or the other elements (Al and Si) neighbouring boron in the periodic table, elemental boron clusters have received relatively little experimental attention<sup>9–13</sup>. The earlier experimental observation of a prominent B<sub>13</sub><sup>+</sup> cluster<sup>9</sup> has stimulated a number of theoretical investigations on the structures of small boron clusters<sup>14–24</sup>. As first proposed in 1994<sup>19</sup>, surprisingly B<sub>12</sub><sup>+</sup> and B<sub>13</sub><sup>+</sup>, as well as their neutral counterparts, have been shown computationally to be planar or quasi-planar<sup>20–24</sup>, very different from the 3D cages so familiar in bulk boron and its compounds. Thus, it appears that boron and carbon form a set of complementary chemical systems: whereas bulk carbon in its most stable form is characterized by a 2D system (graphite) and carbon clusters are characterized by 3D cages, bulk boron is characterized by 3D cages and boron clusters are characterized by 2D structures. However, the predicted 2D structures of boron clusters have not been confirmed experimentally. Thus, the structures and bonding of elemental boron clusters and their size-dependence surprisingly remain an outstanding question in cluster science.

Structural determination of atomic clusters has been experimentally challenging. Ion-mobility experiments have been shown to be able to yield structural information for atomic clusters when combined with theoretical calculations<sup>25–27</sup>. Photoelectron spectroscopy (PES) of size-selected anions is a powerful experimental technique for probing the electronic structure of atomic clusters and their size evolution. Combining PES and *ab initio* calculation is an effective approach to understanding the novel structures and bonding of atomic clusters<sup>28–31</sup>. However, boron clusters have proved to be challenging for PES studies. Only recently have we been able to obtain high-quality data on these seemingly simple clusters<sup>32,33</sup> as a result of

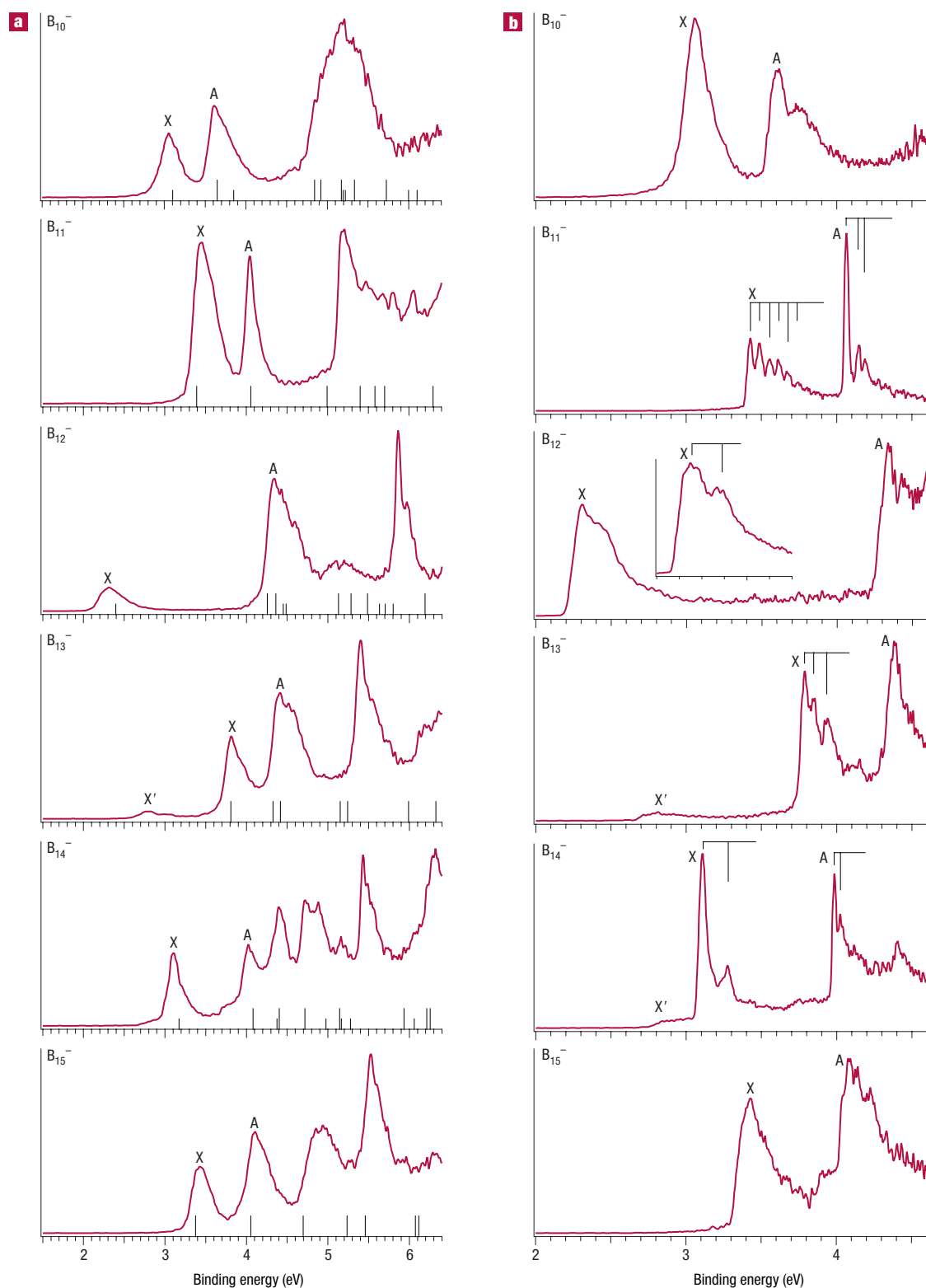


**Figure 1** Photoelectron spectra of  $B_x^-$  ( $x=10-15$ ). **a**, At 193 nm. The vertical bars off the binding energy axis represent the calculated vertical electron detachment energies for the lowest anion structures (see Table 1 and Supplementary Information, Table S1). For even-sized clusters, the shorter bars represent detachment transitions to singlet neutral states, whereas the longer bars represent transitions to triplet final states. **b**, At 266 nm. The inset in the frame of  $B_{12}^-$  shows the spectrum of  $B_{12}^-$  at 355 nm. The vertical lines above the spectra indicate resolved vibrational structures.

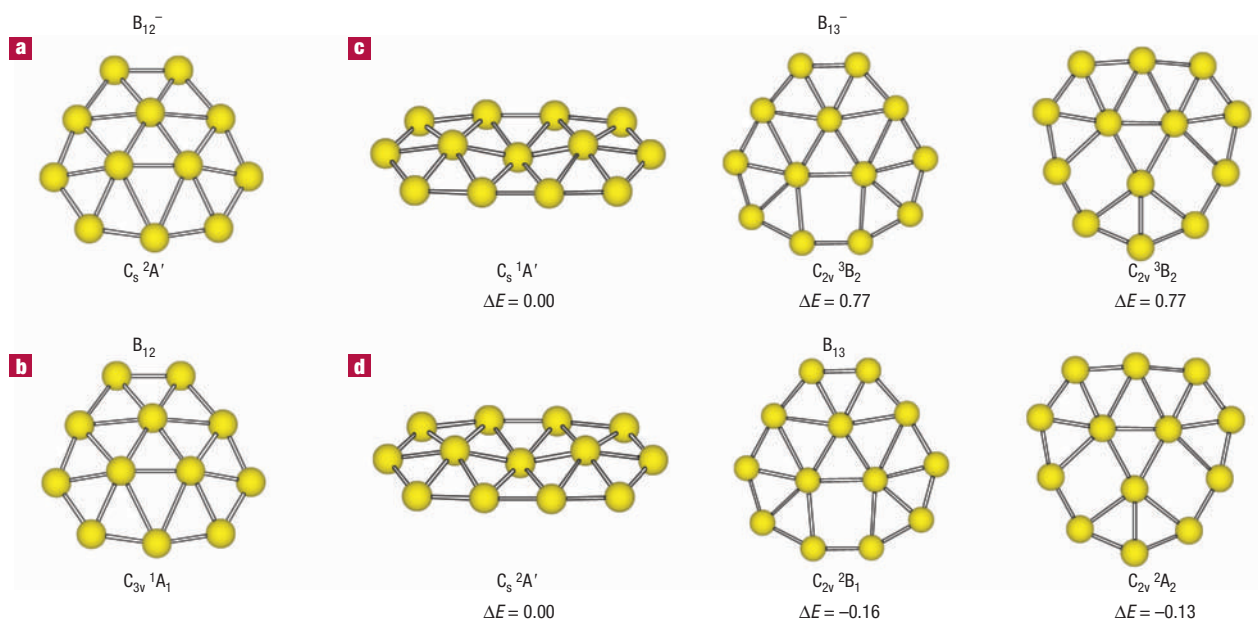


**Figure 2** The low-lying structures of  $B_{12}^-$  and  $B_{13}^-$  and their neutrals. **a, b**, The lowest-energy structure calculated for **a**,  $B_{12}^-$  and **b**,  $B_{12}$ . **c, d**, The three low-lying structures calculated with their relative energies in eV for **c**,  $B_{12}^-$  and **d**,  $B_{13}^-$ .

improved experimental conditions<sup>34</sup>. Here we report a combined PES and theoretical study on boron clusters containing ten to fifteen atoms. We confirm both experimentally and theoretically that these clusters are all dominated by planar or quasi-planar structures and discover most surprisingly that they in fact exhibit aromaticity and antiaromaticity following the well-known Hückel rules, analogous to hydrocarbons. We find that the  $B_{11}^-$  and  $B_{12}$  clusters are unusually stable planar clusters each with six delocalized  $\pi$  electrons, analogous to  $C_5H_5^-$  and  $C_6H_6$  (benzene), respectively.  $B_{10}$  and  $B_{15}^-$  are also aromatic with six and ten  $\pi$  electrons, respectively. The aromatic stabilization induces an extremely large energy gap in  $B_{12}$  between its highest occupied molecular orbital (HOMO) and lowest unoccupied molecular orbital (LUMO).  $B_{13}^-$  and  $B_{14}$  are shown to possess eight delocalized  $\pi$  electrons and are antiaromatic. The elongated shapes of the  $B_{13}^-$  and  $B_{14}$  clusters are due to antiaromaticity, analogous to the square-to-rectangular structural distortion in cyclobutadiene.

## PHOTOELECTRON SPECTROSCOPY

Boron cluster anions were produced by laser vaporization and studied with a magnetic-bottle PES apparatus<sup>32–34</sup>. The PES spectra of  $B_x^-$  ( $x = 10–15$ ) (Fig. 1) revealed well-resolved detachment features for each cluster, representing electronic transitions from the ground state of the anion to the ground and excited states of the neutral clusters. These features can be viewed as ‘fingerprints’ for the anions, and can be used to compare with calculated detachment energies from the anion ground state<sup>28–33</sup>, as shown by the vertical bars in Fig. 1a (see below).

The 266-nm spectra (Fig. 1b) were better resolved with vibrational structures clearly observed for  $B_{11}^-$  to  $B_{14}^-$ . The first vibrational feature of the ground-state transition (X) yielded accurate adiabatic detachment energies (ADEs) for the neutral clusters. Vertical detachment energies (VDEs) were measured from the peak maximum. For the spectra of  $B_{10}^-$  and  $B_{15}^-$ , no vibrational structures were resolved for the X band, and their ADEs were estimated from the threshold. The most striking

observation was for the spectra of  $B_{12}^-$ , revealing an extremely large HOMO–LUMO gap for neutral  $B_{12}$  (2.0 eV as measured from the separation between the X and A bands). The weak low-binding energy feature (X') in the spectra of  $B_{13}^-$  was due to the presence of a low-lying isomer, whose intensity depended on the cluster source conditions. The weak low-binding-energy tail observable in the spectra of  $B_{14}^-$  was also due to potential isomers. The ADE and VDE for the ground-state transition (X) and the VDE of the first excited state (A) are given in Table 1 and compared with theoretical calculations, as shown below.

## PLANAR STRUCTURES OF SMALL BORON CLUSTERS

### THE 12- AND 13-ATOM CLUSTERS

The large HOMO–LUMO gap revealed in the PES spectra of  $B_{12}^-$  indicates that  $B_{12}$  must be electronically extremely stable and should be chemically inert. At first glance, it would be tempting to associate this high stability of the  $B_{12}$  cluster to the icosahedral  $B_{12}$  unit so prevalent in bulk boron crystals and compounds. We carried out an extensive computational search for the structures of  $B_{12}^-$  (Supplementary Information, Fig. S1) and found that the icosahedron-like structure is about 3 eV higher than the lowest-energy structure (Fig. 2a), which is quasi-planar with the three inner atoms slightly out of the plane of the nine peripheral atoms. The neutral  $B_{12}$  ground-state structure was found to be similar to the anion, but with higher symmetry ( $C_{3v}$ , Fig. 2b). The closest low-lying isomer of  $B_{12}^-$  was found to be 1.16 eV higher than the  $C_5$  ground state (Supplementary Information, Fig. S1). Our finding is consistent with previous theoretical calculations about the structures of  $B_{12}$  and  $B_{12}^+$  (refs 20–22).

The 13-atom cluster has been the favourite in previous theoretical efforts, primarily stimulated by the prominent  $B_{13}^+$  peak observed in mass spectra of boron clusters produced from laser vaporization<sup>9</sup>. Its ground-state structure was found to depend on the charge state<sup>24</sup>. The initially anticipated icosahedral structure with a central atom is highly unstable (Supplementary Information, Fig. S1). The low-lying

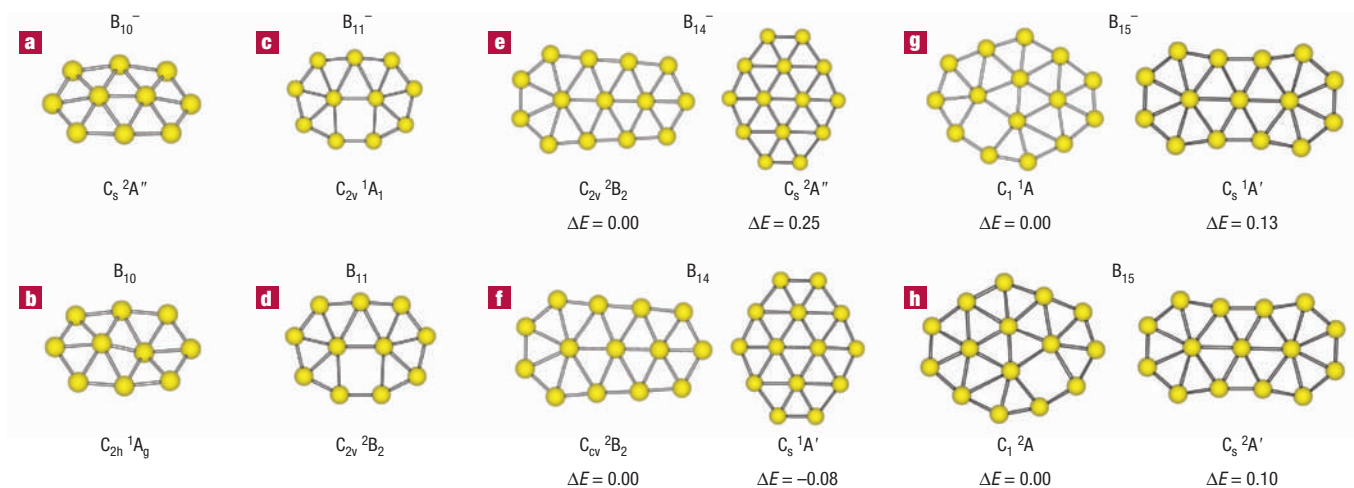


**Figure 3** The low-lying structures of  $B_{10}^-$ ,  $B_{11}^-$ ,  $B_{14}^-$  and  $B_{15}^-$ , and their neutrals. **a–d**, The lowest-energy structures calculated for **a**,  $B_{10}^-$ ; **b**,  $B_{10}$ ; **c**,  $B_{11}^-$ ; **d**,  $B_{11}$ ; **e–h**, The two low-lying structures calculated with their relative energies in eV for **e**,  $B_{14}^-$ ; **f**,  $B_{14}$ ; **g**,  $B_{15}^-$ ; **h**,  $B_{15}$ .

isomers of  $B_{13}^-$  and  $B_{13}$  (Fig. 2c,d) are consistent with previous theoretical results<sup>20–24</sup>. The ground state of  $B_{13}^-$  is a singlet with an elongated quasi-planar structure ( $C_s$ ). Two degenerate low-lying isomers are found for  $B_{13}^-$ , which are both triplet with more circular shapes and slightly different atomic connectivity. For neutral  $B_{13}$ , we computed the three structures corresponding to the three low-lying isomers of  $B_{13}^-$  and found they are all spin doublet, but the two circular structures are slightly more stable than the elongated one.

#### THE 11- AND 10-ATOM CLUSTERS

Our structural searches for  $B_{10}^-$ ,  $B_{11}^-$ ,  $B_{14}^-$  and  $B_{15}^-$  were based on the lowest-energy isomers of  $B_{12}^-$  and  $B_{13}^-$ . There are two ways to build the structures of the 11-atom cluster from the ground-state structure of  $B_{12}^-$ : either by removing an inner atom or a peripheral atom. We found that the former yields the lowest-energy structure for both  $B_{11}^-$  and  $B_{11}$ ; the removal of an inner B atom relieves the strain of the three atoms in the inner circle of the 12-atom cluster and the resulting structures become perfectly planar (Fig. 3c,d). These results differ from previous calculations on  $B_{11}$  and  $B_{11}^+$ , for which only two quasi-planar structures were considered<sup>20–22</sup>. The PES spectra of  $B_{10}^-$  are very similar to those of  $B_{11}^-$ , suggesting that they should have similar geometrical and electronic structures. We built  $B_{10}^-$  by removing a peripheral atom from the lowest-energy structure of  $B_{11}^-$  and obtained the  $C_s$  ground-state structure for  $B_{10}^-$  (Fig. 3a). We tested a number of other 2D structures for  $B_{10}^-$  and found they are all much higher in energy (Supplementary Information, Fig. S1). On electron detachment from the  $C_s$   $B_{10}^-$ , one of the central B atoms is displaced to the other side of the plane, resulting in a  $C_{2h}$   $B_{10}$  neutral (Fig. 3b), which is consistent with previous studies<sup>20–22</sup>.

#### THE 14- AND 15-ATOM CLUSTERS

We considered the 14-atom clusters by inserting an extra atom into the periphery of the three lowest-lying structures of the 13-atom cluster. The elongated structure derived from the ground state of  $B_{13}^-$  becomes the lowest-energy structure of  $B_{14}^-$  (Fig. 3e). A  $C_s$  isomer ( ${}^2A''$ ) is only 0.25 eV higher in energy. For neutral  $B_{14}$  (Fig. 3f), the two structures become nearly degenerate, with the  $C_s$  structure slightly lower in energy by 0.08 eV. We further explored the 15-atom clusters, using the structures of the 14-atom cluster as our starting points. The two structures obtained by inserting an extra atom to the periphery of the

two low-lying planar isomers of the 14-atom cluster are shown in Fig. 3g,h. The ground state for both  $B_{15}^-$  and  $B_{15}$  was found to possess no symmetry ( $C_1$ ) with a somewhat circular shape. The somewhat elongated  $C_s$  structure is a low-lying isomer.

**Table 1** Experimental adiabatic (ADE) and vertical (VDE) detachment energies of  $B_x^-$  ( $x = 10–15$ ) compared with those calculated from the lowest-energy  $B_x^-$  (Figs 2 and 3). All energies are in eV.

		Experimental		Theoretical	
		ADE	VDE	ADE	VDE
$B_{10}^-$	X	2.88 ± 0.09	3.06 ± 0.03	2.84	3.10
	A		3.61 ± 0.04		3.65
$B_{11}^-$	X	3.426 ± 0.010	3.426 ± 0.010	3.27	3.38
	A		4.065 ± 0.010		4.05
$B_{12}^-$	X	2.21 ± 0.04	2.26 ± 0.04	2.25	2.38
	A		4.31 ± 0.05		4.25
$B_{13}^-$	X	3.78 ± 0.02	3.78 ± 0.02	3.69	3.81
	A		4.38 ± 0.06		4.32
$B_{14}^-$	X	3.102 ± 0.010	3.102 ± 0.010	3.14	3.17
	A		3.984 ± 0.010		4.08
$B_{15}^-$	X	3.34 ± 0.04	3.43 ± 0.04	3.24	3.37
	A		4.08 ± 0.06		4.05

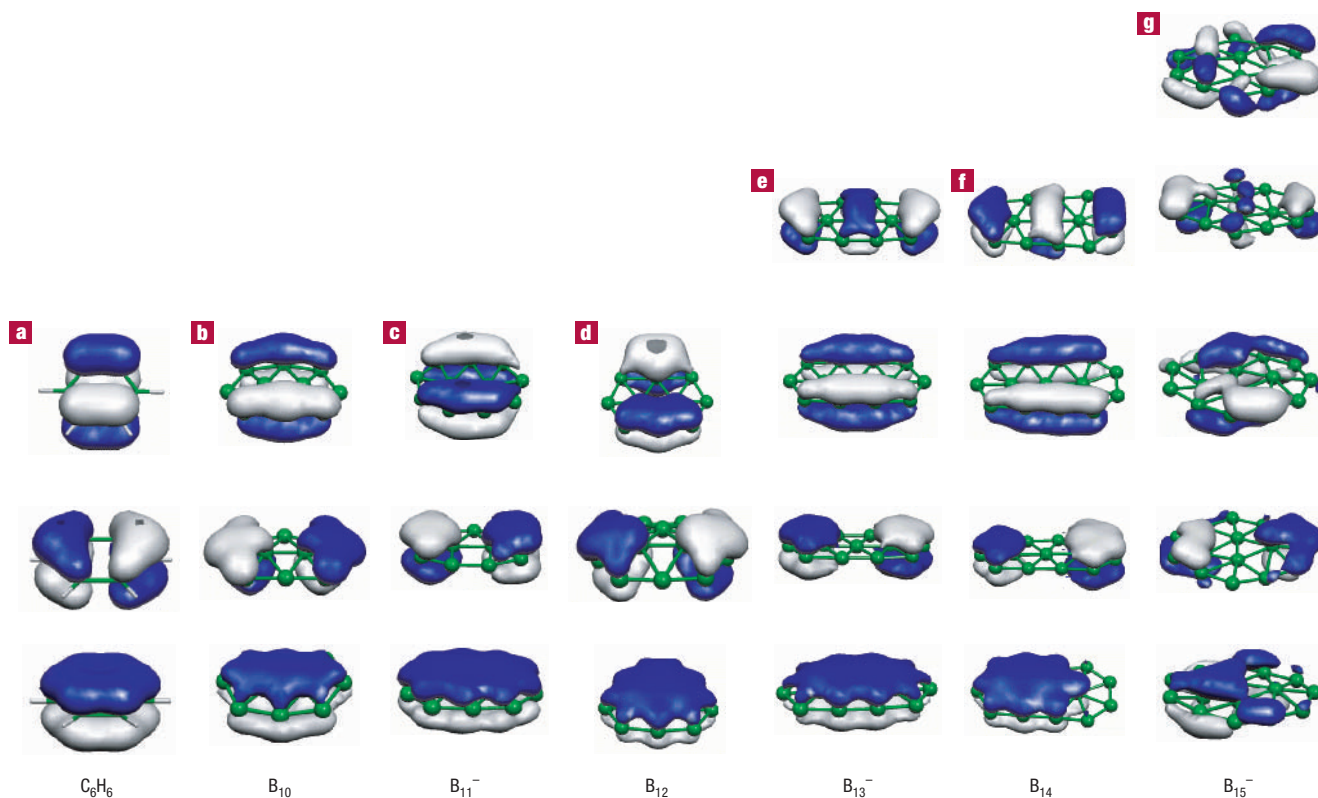


**Figure 4** Comparison of the occupied  $\pi$  molecular orbitals (MOs) of benzene with those of boron clusters. The  $\pi$  MOs are given for: **a**, Benzene; **b**,  $B_{10}$ ; **c**,  $B_{11}^-$ ; **d**,  $B_{12}$ ; **e**,  $B_{13}^-$ ; **f**,  $B_{14}$ ; **g**,  $B_{15}^-$ .

## COMPARISON OF THEORY WITH EXPERIMENT

All the computed VDEs for one-electron transitions from the ground states of the anions, within the energy range of our 193 nm spectrum, are compared with the PES spectrum (Fig. 1a) (numerical values are given in the Supplementary Information, Table S1). The calculated ADE and the first VDE are compared with the experimental data in Table 1. The agreement between the theoretical results and the experimental data are excellent, confirming unequivocally the quasi-planar structures of the boron clusters. (VDEs for the lowest-lying isomer (not shown) were also computed, but they disagree with the experimental spectra (Supplementary Information, Table S1).) The weak low-binding-energy feature (X') in the spectra of  $B_{13}^-$  agrees well with the calculated ADE and VDE for the low-lying isomer (Supplementary Information, Table S1).

The spectral shapes of the first PES band (X) are all consistent with the structural changes from the ground state of the anions to the corresponding neutrals. The structural changes from the ground state of  $B_{11}^-$  to that of  $B_{11}$  are relatively minor and they both have the same  $C_{2v}$  symmetry, explaining why only two vibrational modes are active during photodetachment and responsible for the relatively simple vibrational progressions observed in the 266-nm spectrum (Fig. 1b). The high-frequency mode has a frequency of  $1,040 \pm 50 \text{ cm}^{-1}$ , corresponding primarily to the B–B stretching of the inner two atoms (the calculated frequency is  $1,092 \text{ cm}^{-1}$ , see Supplementary Information, Table S3). The lower-frequency mode has an observed frequency of  $480 \pm 40 \text{ cm}^{-1}$ , which corresponds primarily to the stretching of the peripheral atoms relative to the two inner atoms (the calculated frequency of this mode is  $481 \text{ cm}^{-1}$ ).

## AROMATICITY AND ANTIAROMATICITY IN BORON CLUSTERS

Boron has an electron configuration of  $1s^2 2s^2 2p^1$  and undergoes  $sp^2$  hybridization in most of its compounds. That leaves one empty  $p$ -orbital and renders boron electron-deficient. The chemical bonding of boron is thus dominated by its electron-deficient character and the conventional two-centre two-electron bonds are not favoured<sup>1,2</sup>. Rather, multi-centre bonds predominate in boron chemistry with the three-centre triangular BBB unit becoming a key structural and bonding feature to accommodate the electron-deficiency<sup>35</sup>. Thus in boron materials the boron atoms tend to assume geometries that are based on polyhedra in which triangular faces prevail, such as in the icosahedral  $B_{12}$  unit and  $B_{12}H_{12}^{2-}$ . The planar structures reported here for elemental boron clusters are consistent with the dominance of the BBB three-centre bonding. But, why are the 3D cages so unstable in the elemental boron clusters?

To gain insight into the nature of the bonding in the planar boron clusters, we performed systematic molecular orbital (MO) analyses for each cluster. We found that in addition to the multicentre  $\sigma$  bonding, all the planar boron clusters possess delocalized  $\pi$  bonds, which quite surprisingly follow the  $4n + 2$  and  $4n$  Hückel rules for aromaticity and antiaromaticity, respectively. Figure 4 shows the occupied  $\pi$  MOs for the ground-state structures of  $B_{10}$ ,  $B_{11}^-$ ,  $B_{12}$ ,  $B_{13}^-$ ,  $B_{14}$  and  $B_{15}^-$ . The ground states of all these boron clusters have low spins, so for the even-sized clusters we use the MOs of the neutral clusters because they are closed-shell singlets.  $B_{10}$ ,  $B_{11}^-$  and  $B_{12}$  possess six  $\pi$  electrons each and are aromatic.  $B_{13}^-$  and  $B_{14}$  both possess eight  $\pi$  electrons and are antiaromatic.  $B_{15}^-$  possesses ten  $\pi$  electrons and is

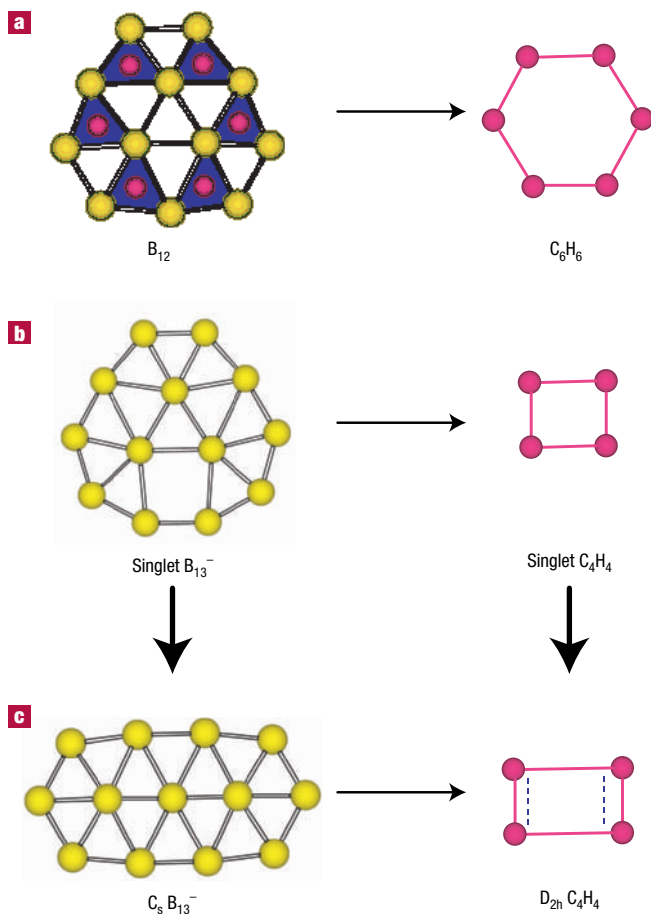


**Figure 5** Analogy of the aromaticity and antiaromaticity between boron clusters and hydrocarbons. **a**, The analogy between the  $\pi$  framework of B<sub>12</sub> and that of benzene. **b**, The unstable B<sub>13</sub><sup>-</sup> and the unstable square C<sub>4</sub>H<sub>4</sub>. **c**, The analogy between elongation of B<sub>13</sub><sup>-</sup> and that of C<sub>4</sub>H<sub>4</sub> due to antiaromaticity.

again aromatic. The boron hydride cage molecules, B<sub>n</sub>H<sub>n</sub><sup>2-</sup> ( $n = 4-12$ ), have been shown to possess 3D aromaticity<sup>36-38</sup>. However, the aromaticity and antiaromaticity in the boron clusters are unique, reminiscent of those in unsaturated polycyclic hydrocarbons. We believe they hold the key for understanding the planarity of these clusters, as suggested previously for the planar B<sub>13</sub><sup>+</sup> cluster<sup>24,39</sup>.

### B<sub>12</sub> AND B<sub>11</sub><sup>-</sup> AND THEIR ANALOGY TO BENZENE AND C<sub>5</sub>H<sub>5</sub><sup>-</sup>

B<sub>12</sub>, as well as B<sub>11</sub><sup>-</sup> and B<sub>10</sub>, has three occupied  $\pi$  MOs, which are nearly identical to those of benzene (Fig. 4a). The structure of B<sub>12</sub> consists of 13 B<sub>3</sub> triangles (Fig. 2b): 12 triangles surround a central B<sub>3</sub>. The C<sub>3v</sub> structure can also be viewed as the fusion of six non-edge-sharing BBB triangles (Fig. 5a). Assuming each of these triangles contributing a  $\pi$  electron and transforming the  $\pi$  framework out of the C<sub>3v</sub> B<sub>12</sub>, we obtain a six-membered ring system of B<sub>3</sub> (Fig. 5a), which is isomorphous to the  $\pi$  framework of benzene. Thus, the similarity between the  $\pi$  MOs of B<sub>12</sub> and benzene is a natural consequence of the analogous  $\pi$  frameworks of the two molecules. The aromatic B<sub>12</sub> can be considered to be the most prototypical aromatic boron cluster, just like benzene in the aromatic hydrocarbons. The extremely large energy gap observed in the PES spectra of B<sub>12</sub><sup>-</sup> confirms the unusual stability of B<sub>12</sub>.

The planar B<sub>11</sub><sup>-</sup> has fewer triangular faces than B<sub>12</sub>, and the  $\pi$ -system formed from the B<sub>3</sub> units can analogously be compared to that of C<sub>5</sub>H<sub>5</sub><sup>-</sup>, a highly aromatic and stable anion with six  $\pi$  electrons. Indeed, our calculation showed that B<sub>11</sub><sup>-</sup> possesses a large HOMO–LUMO gap, indicating that this anionic boron cluster should be highly chemically inert and stable.

### ANTIAROMATIC CLUSTERS, B<sub>13</sub><sup>-</sup> AND B<sub>14</sub>, AND THE STRUCTURAL CONSEQUENCE OF ANTIAROMATICITY

The aromatic clusters, B<sub>11</sub><sup>-</sup>, B<sub>12</sub> and B<sub>15</sub><sup>-</sup>, all have more circular structures. However, the two antiaromatic clusters, B<sub>13</sub><sup>-</sup> and B<sub>14</sub>, are elongated. This structural elongation is reminiscent of the square-to-rectangular structural distortion in the antiaromatic cyclobutadiene (Fig. 5b,c), which possesses two localized  $\pi$  bonds<sup>40</sup>. Figure 4 shows that the nodal properties of the  $\pi$  MOs in boron clusters are similar to those in hydrocarbons. While the first  $\pi$ -MO ( $\pi_0$ ) has zero node, each subsequent degenerate or near-degenerate pair of  $\pi$ -MOs comes with increasing number of nodes, that is, the first pair ( $\pi_1$ ) has one node and the second pair ( $\pi_2$ ) has two nodes, and so on. Hence, the number of  $\pi$  electrons in the planar boron clusters renders the system aromatic or antiaromatic according to the  $4n + 2$  and  $4n$  Hückel rules, as well as dictating their geometrical shapes, in exactly the same way as in the hydrocarbons.

For the aromatic systems with six or ten  $\pi$  electrons, both components of the frontier  $\pi$  MOs are occupied, yielding the somewhat more circular structures. For clusters with  $4n$   $\pi$  electrons (B<sub>13</sub><sup>-</sup> and B<sub>14</sub>), there are not enough  $\pi$  electrons to completely fill a near-degenerate  $\pi$ -MO pair of a given node. In these cases there are two possibilities. If each component of the  $\pi$ -MO pair is occupied with one electron, resulting in a triplet state, the system is again aromatic<sup>41</sup> and should be circular, as indeed found in the two low-lying isomers of B<sub>13</sub><sup>-</sup> (Fig. 2c). Alternatively, if only one component of the  $\pi$ -MO pair is occupied, a structural elongation ensues, as dictated by the shape of the MO. In planar unsaturated hydrocarbons, antiaromaticity induces bond localization (Fig. 5c)<sup>40</sup>. Our analysis explains the stability of B<sub>13</sub><sup>+</sup> and its enhanced abundance in mass spectra of positively charged boron clusters<sup>9</sup>. On removal of two  $\pi$  electrons from B<sub>13</sub><sup>-</sup>, the resulting B<sub>13</sub><sup>+</sup> possesses only six  $\pi$  electrons and is transformed into a highly aromatic molecule as recognized previously<sup>24,39</sup>, and it should favour a more circular ground-state structure, which is indeed the case.

The Hückel rules for aromaticity and antiaromaticity were derived for monocyclic systems<sup>42</sup>. It is surprising that they are so applicable for the planar boron clusters. However, the  $\pi$  MOs for the larger boron clusters also show some differences from the hydrocarbons. They seem to be localized on certain parts of the clusters. For example, the  $\pi_0$  MO of B<sub>14</sub> is delocalized on one side of the cluster (Fig. 4f) and all the  $\pi$  MOs of B<sub>15</sub><sup>-</sup> appear ‘fragmented’ in different parts of the cluster. Therefore, for larger boron clusters, the Hückel rules may not apply.

### IMPLICATIONS AND PERSPECTIVES

We provide the first experimental confirmation of the planar or quasi-planar structures of boron clusters in the 10- to 15-atom size range, and find that the planarity is due to the delocalization of the  $\pi$  electrons in 2D, which also renders aromaticity and antiaromaticity to the boron clusters analogous to planar hydrocarbons. The electron deficiency of boron and the resulting multi-centre bonding leave no dangling bonds in such 2D structures, whereas the tendency to terminate the dangling bonds and the strong C–C multiple bond give entirely different morphologies for small carbon clusters: from linear to cyclic to the fullerene cage structures. Larger boron clusters can be expected to maintain the 2D growth patterns<sup>43,44</sup>. However, the fragmentation (or

localization) of the  $\pi$  orbitals in different parts of the planar structure in the large clusters may eventually make the planar structure less favourable and lead to the appearance of 3D structures<sup>44</sup>. When this 2D-to-3D transition will commence and at what size the icosahedral  $B_{12}$  unit will prevail remain unknown, and should represent significant future research opportunities. The aromatic  $B_{11}^-$  and  $B_{12}$  and their anticipated chemical stability may suggest the possibility of using them to form full or half sandwich-type compounds, such as those formed by  $C_5H_5^-$  and  $C_6H_6$ . Considering the rich chemistry of boron clusters and the wide morphologies of bulk boron compounds, we expect that there may be more surprises in the structures and bonding patterns of larger elemental boron clusters.

## METHODS

### PHOTOELECTRON SPECTROSCOPY

Boron cluster anions were produced by laser vaporization of a disk target made of enriched  $^{10}B$  isotope (99.75%)<sup>32,33</sup>. The clusters were entrained in a helium carrier gas and underwent a supersonic expansion to form a collimated cluster beam. The negatively charged clusters were analyzed with a time-of-flight mass spectrometer. Clusters of interest were mass-selected before irradiation by a laser beam. Photoelectron spectra were measured with a home-built magnetic-bottle PES apparatus, which has an electron-energy resolution of  $\Delta E_k/E_k \sim 2.5\%$ , that is, 25 meV for 1 eV electrons<sup>32–34</sup>. All equipment was home-built.

### THEORETICAL METHODS

Theoretical calculations on the anionic and neutral boron clusters were performed by density functional theory using the Amsterdam Density Functional (ADF 2002.3) program<sup>45</sup>. The gradient-corrected Perdew–Wang 1991 (PW91) functional was chosen to account for the exchange and correlation interactions<sup>46</sup>. The Slater basis sets with quality triple-zeta plus d- and f-type polarization functions (TZ2P) were used for the valence space and the  $1s^2$  atomic core of B was treated by the frozen-core approximation. All the geometry structures were fully optimized under given symmetry and the nature of the stationary points was checked by vibrational frequency calculations. As some of the structures have quite flat potential-energy surfaces, tight convergence criteria ( $10^{-4}$  Hartree per ångström) for energy gradients were adopted in geometry optimizations. The electron-detachment energies for the open-shell anions were calculated through the energy differences of the excitation energies of the neutral species calculated by time-dependent density functional theory<sup>47</sup> and the ground-state energy of the anions, whereas those for the close-shell anions were calculated through the  $\Delta$ SCF (self-consistent field) method<sup>48</sup>.

Received 15 May 2003; accepted 3 October 2003; published 9 November 2003

## References

- Lipscomb, W. L. *Boron Hydrides* (W. A. Benjamin, New York, 1963).
- Meuterties, E. L. (ed.) *Boron Hydride Chemistry* (Academic, New York, 1975).
- Cotton, F. A., Wilkinson, G., Murillo, C. A. & Bochmann, M. *Advanced Inorganic Chemistry* 6th edn (Wiley, New York, 1999).
- Smith, K. Boron's molecular gymnastics. *Nature* **348**, 115–116 (1990).
- Jemmis, E. D., Balakrishnarajan, M. M. & Pancharatna, P. D. Electronic requirements for macropolyhedral boranes. *Chem. Rev.* **102**, 93–144 (2002).
- Proceedings of the 13<sup>th</sup> international symposium on boron, borides, and related compounds (ISBB'99). *J. Solid State Chem.* **154** (special issue), 1–320 (2000).
- Perkins, C. L., Trenary, M. & Tanaka, T. Direct observation of  $(B_{12})(B_{12})_{12}$  supericosahedra as the basic structural element in  $YB_{60}$ . *Phys. Rev. Lett.* **77**, 4772–4775 (1996).
- Hubert, H. *et al.* Icosahedral packing of  $B_{12}$  icosahedra in boron suboxide ( $B_6O$ ). *Nature* **391**, 376–378 (1998).
- Hanley, L. & Anderson, S. L. Production and collision-induced dissociation of small boron cluster ions. *J. Phys. Chem.* **91**, 5161–5163 (1987).
- Hanley, L., Whitten, J. L. & Anderson, S. L. Collision-induced dissociation and ab initio studies of boron cluster ions: determination of structure and stabilities. *J. Phys. Chem.* **92**, 5803–5812 (1988).
- Hintz, P. A., Sowa, M. B., Ruatta, S. A. & Anderson, S. L. Reactions of boron cluster ions ( $B_n^+$ ,  $n = 2–24$ ) with  $N_2O$ : NO versus NN bond activation as a function of size. *J. Chem. Phys.* **94**, 6446–6458 (1991).
- Sowa-Resat, M. B., Smolanoff, A. L., Lapicki, A. & Anderson, S. L. Interaction of small boron cluster ions with HF. *J. Chem. Phys.* **106**, 9511–9522 (1997).
- La Placa, S. J., Roland, P. A. & Wynne, J. J. Boron clusters ( $B_n$ ,  $n = 2–52$ ) produced by laser ablation of hexagonal boron nitride. *Chem. Phys. Lett.* **190**, 163–168 (1992).
- Kawai, R. & Weare, J. H. Instability of the  $B_{12}$  icosahedral cluster: rearrangement to a lower energy structure. *J. Chem. Phys.* **95**, 1151–1159 (1991).
- Kwai, R. & Weare, J. H. Anomalous stability of  $B_{13}^+$  clusters. *Chem. Phys. Lett.* **191**, 311–314 (1992).
- Ray, A. K., Howard, I. A. & Kanal, K. M. Structure and bonding in small neutral and cationic boron clusters. *Phys. Rev. B* **45**, 14247–14255 (1992).
- Bonacic-Koutecky, V., Fantucci, P. & Koutecky, J. Quantum chemistry of small clusters of elements of group Ia, Ib, and IIa: fundamental concepts, predictions, and interpretation of experiments. *Chem. Rev.* **91**, 1035–1108 (1991).
- Kato, H., Yamashita, K. & Morokuma, K. *Ab initio* MO study of neutral and cationic boron clusters. *Chem. Phys. Lett.* **190**, 361–366 (1992).
- Boustani, I. Systematic LSD investigation on cationic boron clusters –  $B_n^+$  ( $n = 2–14$ ). *Int. J. Quantum Chem.* **52**, 1081–1111 (1994).
- Boustani, I. Structure and stability of small boron clusters. A density functional theoretical study. *Chem. Phys. Lett.* **240**, 135–140 (1995).
- Ricca, A. & Bauschlicher, C. W. The structure and stability of  $B_n^+$  clusters. *Chem. Phys.* **208**, 233–242 (1996).
- Boustani, I. Systematic *ab initio* investigation of bare boron clusters: determination of the geometrical and electronic structures of  $B_n$  ( $n = 2–14$ ). *Phys. Rev. B* **55**, 16426–16438 (1997).
- Gu, F. L., Yang, X., Tang, A. C., Jiao, H. & Schleyer, P. v. R. Structure and stability of  $B_{13}^+$  clusters. *J. Comput. Chem.* **19**, 203–214 (1998).
- Fowler, J. E. & Ugalde, J. M. The curiously stable  $B_{13}^+$  cluster and its neutral and anionic counterparts: the advantages of planarity. *J. Phys. Chem. A* **104**, 397–403 (2000).
- Heldon, G. V., Kemper, P. R., Gotts, N. G. & Bowers, M. T. Isomers of small carbon cluster anions: linear chains with up to 20 atoms. *Science* **259**, 1300–1302 (1993).
- Ho, K. M. *et al.* Structures of medium-sized silicon clusters. *Nature* **392**, 582–585 (1998).
- Furche, F. *et al.* The structures of small gold cluster anions as determined by a combination of ion mobility measurements and density functional calculations. *J. Chem. Phys.* **117**, 6982–6990 (2002).
- Kronik, L., Fromherz, R., Ko, E. J., Gantefor, G. & Chelikowsky, J. R. Highest electron affinity as a predictor of cluster anion structures. *Nature Mater.* **1**, 49–53 (2002).
- Massobrio, C., Pasquarello, A. & Car, R. First principles study of photoelectron spectra of  $Cu_n^-$  clusters. *Phys. Rev. Lett.* **75**, 2104–2107 (1995).
- Boldyrev, A. I. & Wang, L. S. Beyond classical stoichiometry: experiment and theory. *J. Phys. Chem. A* **105**, 10759–10775 (2001).
- Li, J., Li, X., Zhai, H. J. & Wang, L. S.  $Au_{39}$ : a tetrahedral cluster. *Science* **299**, 864–867 (2003).
- Zhai, H. J., Wang, L. S., Alexandrova, A. N. & Boldyrev, A. I. Electronic structure and chemical bonding of  $B_5^-$  and  $B_5$  by photoelectron spectroscopy and *ab initio* calculations. *J. Chem. Phys.* **117**, 7917–7924 (2002).
- Alexandrova, A. N. *et al.* Structure and bonding in  $B_6^-$  and  $B_6$ : planarity and antiaromaticity. *J. Phys. Chem. A* **107**, 1359–1369 (2003).
- Wang, L. S. & Li, X. in *Clusters and Nanostructure Interfaces* (eds Jena, P., Khanna, S. N. & Rao, B. K.) 293–300 (World Scientific, New Jersey, 2000).
- Lipscomb, W. N. Three-center bonds in electron-deficient compounds. The localized molecular orbital approach. *Acc. Chem. Res.* **6**, 257–262 (1973).
- Aihara, J. Three-dimensional aromaticity of polyhedral boranes. *J. Am. Chem. Soc.* **100**, 3339–3342 (1978).
- King, R. B., Dai, B. & Gimarc, B. M. Three-dimensional aromaticity in deltahedral borane anions: comparison of topological and computational approaches. *Inorg. Chim. Acta* **167**, 213–222 (1990).
- Schleyer, P. v. R., Najafian, K. & Mebel, A. M. The large closo-borane dianions,  $B_nH_n^{2-}$  ( $n = 13–17$ ), are aromatic, why are they unknown? *Inorg. Chem.* **37**, 6765–6772 (1998).
- Aihara, J.  $B_{13}^+$  is highly aromatic. *J. Phys. Chem. A* **105**, 5486–5489 (2001).
- Breslow, R. Antiaromaticity. *Acc. Chem. Res.* **6**, 393–398 (1973).
- Baird, N. C. Quantum organic photochemistry. II. Resonance and aromaticity in the lowest  $^3\pi\pi^*$  state of cyclic hydrocarbons. *J. Am. Chem. Soc.* **94**, 4941–4948 (1972).
- Choi, C. H. & Ketzec, M. Bond length alternation and aromaticity in large annulenes. *J. Chem. Phys.* **108**, 6681–6688 (1998).
- Boustani, I. New quasi-planar surfaces of bare boron. *Surf. Sci.* **370**, 355–363 (1997).
- Boustani, I. *Ab initio* study of  $B_{32}$  clusters: competition between spherical, quasiplanar and tubular isomers. *Chem. Phys. Lett.* **311**, 21–28 (1999).
- ADF 2002, SCM, Theoretical Chemistry, Vrije Universiteit, Amsterdam, The Netherlands (<http://www.scm.com>)
- Perdew, J. P. & Wang, Y. Accurate and simple analytic representation of the electron-gas correlation energy. *Phys. Rev. B* **45**, 13244–13249 (1992).
- van Gisbergen, S. J. A., Snijders, J. G. & Baerends, E. J. Implementation of time-dependent density functional response equations. *Comput. Phys. Commun.* **118**, 119–138 (1999).
- Ziegler, T., Rauk, A. & Baerends, E. J. On the calculation of multiplet energies by the Hartree–Fock–Slater method. *Theor. Chim. Acta* **43**, 261–269 (1977).

### Acknowledgements

This work was supported by the US National Science Foundation (DMR-0095828) and partly by the Petroleum Research Fund administered by the American Chemical Society and performed at the EMSL, a national scientific user facility sponsored by Department of Energy's (DOE) Office of Biological and Environmental Research and located at the Pacific Northwest National Laboratory, operated for DOE by Battelle. All the calculations were performed using supercomputers at EMSL Molecular Science Computing Facility.

Correspondence and requests for materials should be addressed to L.S.W.

Supplementary Information accompanies the paper on [www.nature.com/naturematerials](http://www.nature.com/naturematerials)

### Competing financial interests

The authors declare that they have no competing financial interests.